DC Resistivity Measurements on the Sea Ice near Pond Inlet, N.W.T. (Baffin Island)

By F. Thyssen, H. Kohnen, M. V. Cowan and G. W. Timco *

Summary: Extensive dc-resistivity measurements were carried out in May and June 1972 near Pond Inlet, N. W. T. to determine the resistivity and the anisotropy of the sea ice.
The sea ice proved to be transversely isotropic with regard to dc currents. The coefficient of anisotropy of undisturbed ice is approximately $\lambda = 0,26$. λ increased up to 1 in heavily disturbed parts of the ice cover. Ice thicknesses, determined from the dc-soundings without taking into account anisotropy, were too small compared with the true thicknesses determined from drilling. The average resistivity of the sea ice decreased significantly during the observation period according to the increase of the brine volume. The conductivity of the ice is controlled by this brine content since the ice matrix has an extremly low conductivity. The relation between the resistivity and the brine volume is compared with a model of conductivity in porous media.

Zusammenfassung: Während der Monate Mai und Juni 1972 wurden auf dem Meereis bei Pond Inlet, N.W.T., umfangreiche Schlumbergersondierungen zur Bestimmung des spezifischen Widerstandes und der Anisotropie des Eises durchgeführt.
Das Meereis erwies sich im wesentlichen als transversalanisotrop. Der Anisotropiefaktor betrug im ungestörten Eis etwa 0,26 und stieg in stark gestörten Bereichen der Eisdecke bis auf nahezu 1. Die aus den Schlumbergersondierungen abgeleiteten Eisdicken waren ohne Berücksichtigung der Anisotropie entsprechend zu gering im Vergleich mit den erbohrten Mächtigkeiten.
Der mittlere spezifische Widerstand des Eises zeigt eine Abnahme über die Meßperiode infolge der Temperaturerhöhung und der damit verbundenen Zunahme an Salzlösung in den Poren. Die Leitfähigkeit des Meereises wird durch den Gehalt als Salzlösung bestimmt. Im Vergleich dazu kann die Eismatrix als nichtleitend behandelt werden. Die Abhängigkeit des Widerstandes vom Lösungsgehalt wird mit einem Modell der DC-Leitfähigkeit in porösen Medien verglichen.

Introduction

The dc resistivity of sea ice has been studied in situ only sporadically in the past. Because it is a basic physical parameter of the sea ice, extensive dc resistivity measurements were carried out near Pond Inlet N. W. T. during May and June 1972 as part of the Canadian Arctic Channel Project.

The resistivity of sea ice depends chiefly on the salinity, the distribution of brine inclusions and the crystal texture of the ice. Since mechanical, optical as well as electromagnetic properties depend also on these parameters it seemed important to us to study the variation of the resistivity with time and temperature.

Field measurements

Schlumberger geoelectric sounding is a suitable method of measuring the in situ resistivity of sea ice. Determining the resistivity from samples would have the disadvantage that at ice temperatures near the melting point (Table 2) brine drainage would take
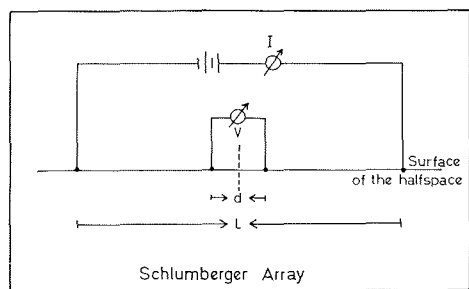

Fig. 1: The Schlumberger configuration.
Abb. 1: Die Schlumberger-Anordnung.

* Prof. Dr. Franz Thyssen and Dr. Heinz Kohnen, Institut für Geophysik der Universität, D 44 Münster (Westf.), Gievenbecker Weg 61.
Dr. Michael V. Cowan, Dept. of Physics, Vanier College, Montreal, P. Q. (Canada).
Garry W. Timco, M. Sc., Dept. of Geophysics, University of Western Ontario, London, Ont. (Canada).

place immediately. The Schlumberger configuration (Fig. 1) was therefore applied using steel rods as current probes and non-polarizable electrodes (thin copper rods in saturated copper sulphate solution ($CuSO_4$), for measuring the potential difference. A maximum spacing of the current electrodes of about 7m proved to be sufficient to determine the resistivity distribution within the ice cover. The aparent resistivity is calculated from

$$1)\ \varrho_s = \frac{\pi}{4}\ \frac{V}{I}\ \frac{L^2 - d^2}{d}$$

(Schlumberger configuration)

where ϱ_s is the apparent resistivity, V ist the potential difference, I is the current, L the current electrode spacing and d is the voltage electrode spacing. ϱ_s is plotted against L/2 in log-log paper (Fig. 3) to evaluate the thickness of the ice cover as well as the resistivity.
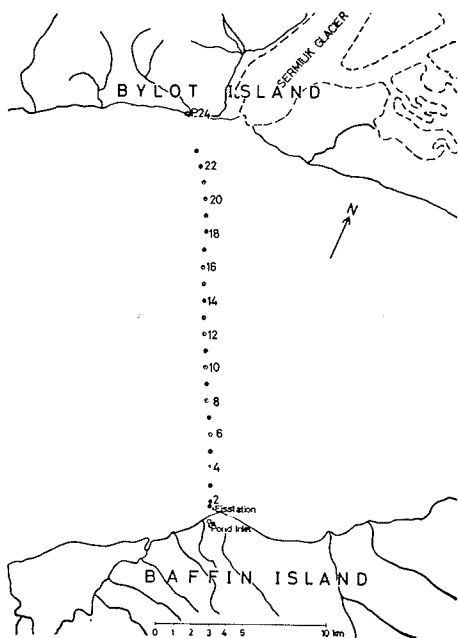

Fig. 2: Map of the Pond Inlet area showing the profile and the survey sites.
Abb. 2: Lageplan des Profils und der Schlumbergersondierungen bei Pond Inlet.

Soundings were made at 22 sites (P2 to P23) on the profile from Pond Inlet to Bylot Island separated by approximately 1 km (Fig. 2). The soundings were repeated (Fig. 5) at intervals of two weeks to observe the resistivity variation with time. During the first run cross soundings, angled at 90° to each other, were carried out at the sites P2 to P10 looking for azimuthal variations of the resistivities.

The sea ice is highly anisotropic with regard to its conductivity. To study this effect a pit was dug into the unrafted ice near P2 and the apparent resistivity was measured perpendicular and parallel to the ice surface.

The dc anisotropy of the sea ice

Taking into account the considerable scatter of the apparent resistivities even between adjacent points no significant azimuthal variation of ϱ_s was found from the cross sound-
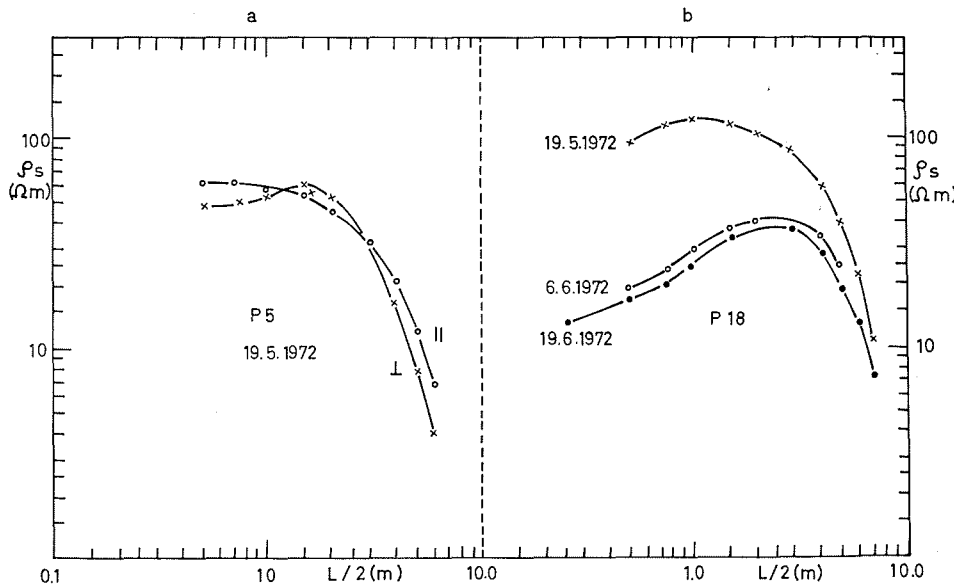
118

Fig. 3: Examples of resistivity curves ϱ_s (L/2): a) from the cross sounding at P5, b) from different runs at P18.

Abb. 3: Beispiele von Sondierungskurven ϱ_s (L/2): a) Kreuzprofil bei P5, b) drei Messungen bei P18.

ings (Fig. 3a) at 12 different sites. Therefore, we may conclude that the ice cover is either isotropic or transversely isotropic.

Howerer, assuming that through about almost the whole ice cover the cylindrical brine pockets are arranged vertically we may treat the ice plate as a homogeneous, transversely isotropic single layer above the infinite medium of sea water. The apparent resistivity in such a medium is given by (Bhattacharya and Patra, 1968):

2) $$\varrho_s = \frac{\varrho_m}{[1 + (\lambda^2-1)\,\sin^2\gamma\,\sin^2\alpha]^{1/2}}$$

$\rho_m = \sqrt{\rho_t \cdot \rho_l}$ (mean resistivity)

$\lambda = \sqrt{\rho_t/\rho_l}$ (coefficient of anisotropy)

ϱ_l is the resistivity parallel and ϱ_t the resistivity perpendicular to the surface.

γ and α are angles related to the geometry of the anisotropic medium. In a stratified or layered medium (microstratification) α ist the dip angle between the surface and the layers whereas γ is the angle between the electrode array and the strike direktion. The main axis of such anisotropy is perpendicular to the stratification. In sea ice, the vertical alignment of the brine cells corresponds to the main axes of anisotropy and, therefore, for Schlumberger soundings on the surface of unrafted ice, $\alpha = O$ and thus $\varrho_s = \varrho_m$ regardless of γ. Measurements on the pit walls have a different geometry with regard to α and γ. The main axis of anisotropy is parallel to the pit wall and the vertical electrode array is perpendicular to the strike direction. Thus $\alpha = \pi/2$, $\gamma = \pi/2$ and it follows:

$$\varrho_{ts} = \frac{\varrho_m}{\lambda} = \varrho_l$$

119

which is called the "paradox of anisotropy". With the array parallel to the surface on the pit walls ($\gamma = O$, $\alpha = \pi/2$) we obtain again $\varrho_{ls} = \varrho_m$. The measurements on the pit walls (June 8) were carried out with two constant electrode arrays (L = 120 cm and L = 80 cm). Twenty single measurements in each direction yielded $\varrho_l = 221$ Ω m, $\varrho_m = 60$ Ω m and $\varrho_t = 16$ Ω m provided that any brine drainage out of the upper centimeters of the wall can be neglected because the penetration of the main current is much deeper. From these values $\lambda = 0{,}26$ results for unrafted ice.

The determination of the ice thickness from the apparent resistivities without considering the anisotropy gives the "effective thickness" h_e. It is easy to show that $h_e = \lambda H$, assuming that λ is constant over the entire depth. H is the true thickness and was determined at each station by drilling. In Figure 4a, the effective thickness h_e and the true thickness H are plotted against the profile. Since the effective thickness did not show any significant variation with time (Table 1) the average of the three runs is taken. h_e is markedly smaller than H as expected from the pit studies. The coefficient of anisotropy, calculated from the thicknesses h_e and H is plotted in the same graph (Fig. 4b). These coefficients are generally greater than λ obtained from the pit studies. In spite of the considerable scatter there are systematic differences along the profile which allow one to distinguish three different regions. λ is smallest in region II ($\approx 0{,}3$)
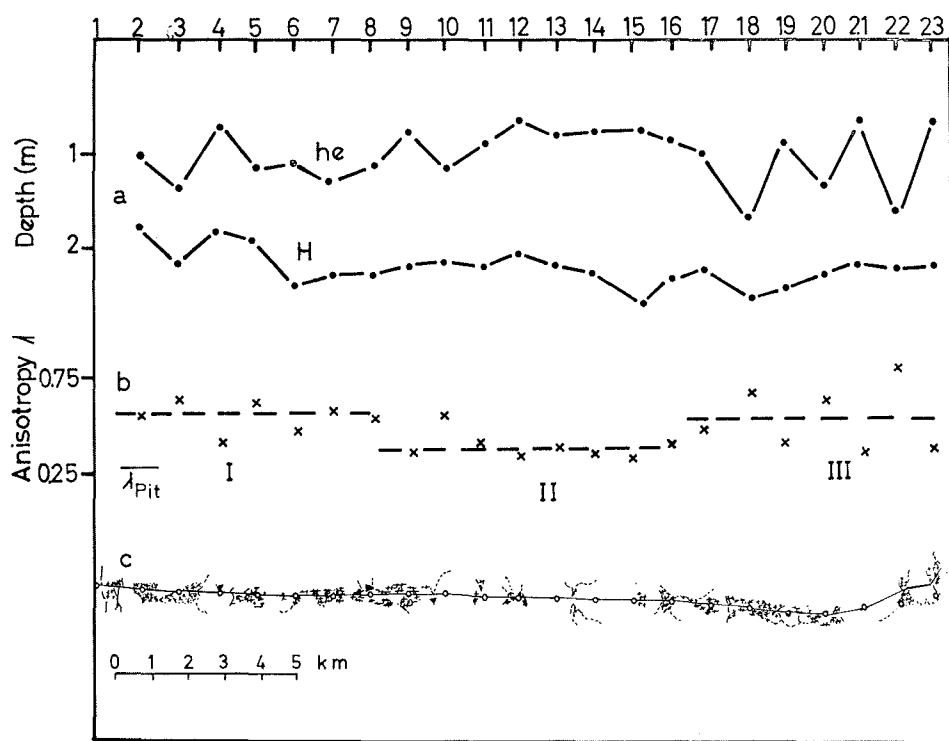

Fig. 4: a) Ice thickness h_e determined from the Schlumberger soundings without taking into account the anisotropy and true ice thickness H obtained from drilling; b) the coefficient of anisotropy; c) the ice surface structure after Walter and Blewett (1972) along the survey profile (dotted areas and crosses represent rafted ice and ridges).

Abb. 4: a) Eismächtigkeiten h_e, die unter Vernachlässigung der Anisotropie aus den Schlumbergersondierungen gewonnen wurden, und die erbohrten Mächtigkeiten H; b) der Anisotropiefaktor; c) die Struktur der Eisoberfläche nach Walter und Blewett (1972) längs des Profils von Pond Inlet nach Bylot Island (Kreuze und gepunktete Flächen markieren Ridge-Zonen und stark gestörtes Eis).

120

which correponds to a rather undisturbed, unrafted part of the ice cover (Fig. 4c), whereas the values of region I and III were obtained in areas of rafted ice with frequent ridges.

The scatter of λ is caused by the scatter in h_e which is due chiefly to inhomogeneities of the ice cover in the immediate vicinity of the soundings, These inhomogeneities are of various origins. Ridges and rafted ice close to the electrode array as well as fracturing of the ice alter the "plane layer conditions" required for the Schlumberger sounding. An uneven bottom morphology with considerable amplitudes from ca 5% up to ca 50% of the total ice trickness yields the same effect. Such morphology is often met and hard to detect from the surface because the ice cover is locally not necessarily in isostatic equilibrium. Finally, there are fractures and cracks filled with sea water affecting seriously the resistivities and consequently the resistivity curves.

All these inhomogeneities act to disorient the normal anisotropy direction and tend to increase the coefficient of anisotropiy. The values from our measurements lie in the range $0,26 < \lambda < 1$ and reflect this tendency. From the pit and surface studies we may conclude that the coefficient of anisotropy of homogeneous, undisturbed sea ice is approximately 0,26 and that any inhomogeneities decrease the anisotropy and make disturbed regions behave like isotropic ice with regard to its conductivity.

Variations in the brine volume due to temperature variations did not influence noticeably the anisotropy as seen from the variations in the effective thickness of the three runs (Table 1). Due to the great scatter in λ it is obvious that Schlumberger sounding is not an appropriate method for surveying the ice thickness.

The resistivities discussed in the following section represent the mean resistivities ϱ_m.

Run	$\overline{\varrho_{m1}}$ [Ωm]	$\overline{\varrho_{m2}}$ [Ωm]	$\overline{h_e}$ [m]
16.—19. 5.	112 ± 65	176 ± 90	0,99 ± 0,36
3.— 6. 6.	46 ± 25	136 ± 67	0,96 ± 0,35
15.—21. 6.	30 ± 12	76 ± 41	1,10 ± 0,44

Tab. 1: Resistivities and ice thickness averaged from the results of the 22 soundings of each run (the anisotropy effect is not taken into account). The scatter of the mean values is also listed.
Tab. 1: Widerstände und Eismächtigkeiten, gemittelt aus den Resultaten der 22 Sondierungen jeder Meßserie ohne Berücksichtigung der Anisotropie. Ferner aufgeführt ist die Streuung der Mittelwerte.

The resistivity and its dependence on brine volume variations

All curves of the apparent resistivities show the same typical feature (Fig. 3b). First, there is a rise of the apparent resistivities with distance and than a rapid decrease due to the low resistivity of the underlying sea water. Simplified, this feature corresponds to a three-layer-case. One electrode array was extended to L = 40 m. From 32 m onwards, ϱ_s remained constant giving 0,40 Ω m as the resistivity of the sea water at a salinity of 32%. The resistivity curves are interpreted using theoretical master curves along with "auxiliary point charts" (Deppermann et al. 1961). Resistivities and effective thickness h_e are obtained by fitting the field data to the theoretical curves. Since the major part of the experimental curves correponds to a three-layer-case this model is adopted as approximation of the resistivity distribution. Of course, the fact that the resistivity of the upper layer is generally lower than the resistivity of the lower layer is hard to explain. A brine drainage from the lower layer cannot be responsible because the drainage in this period is fairly compensated by the increase in brine due to the temperature increase. (The conductivity of a semiconductor with interconnected pore space like the sea ice depends primarily on the electrolyte content of the pores.) Also the fact that the electrodes were buried and not at the surface as required by the theory is insufficient to explain the increase in ϱ_s by occasionally more than 100%. Howerer,

there is evidence (S. F. Ackley et al., 1974) that the cylindrical brine cells are arranged parallel to the surface in the upper centimeters of the sea ice which is due to the fact that the position of the long axes of the brine pocket depends on the growth rate of the ice and is perpendicular to the c-axes of the ice crystals. Such a small top layer with horizontal stratification of the brine pockets could drop the resistivity of the upper part significantly (see the part on the anisotropy). The transition from horizontal to vertical alignment of the brine cells is gradual and a continuous variation of the resistivity is most likely. This effect could be enhanced by the presence of meltwater at the snow-ice interface and by relative brine content maxima which may occur at shallow and inter-
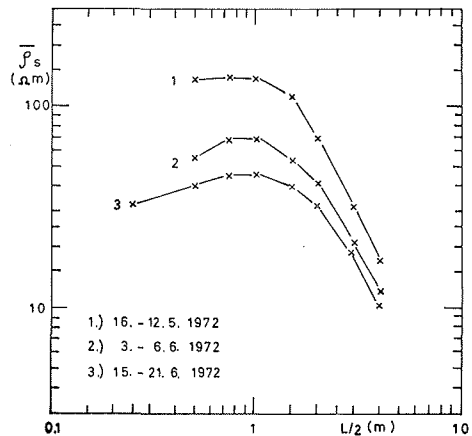

Fig. 5: $\overline{\varrho}_s$-curves obtained by averaging the 22 ϱ_s-curves of each run.

Abb. 5: $\overline{\varrho}_s$-Kurven, gemittelt aus den 22 Sondierungen jeder Meßserie.

mediate depths due to the daily and seasonally varying temperature profile within the ice, especially in May and June when the ice cover is warming up. Thus, the three layer model is certainly over-simplifying but nevertheless appropriate for the succeeding investigations.

Since there were no drastic resistivity jumps between P2 and P 23 (Fig. 7) we may conclude by the aid of the salinities which were about almost the same (Fig. 6) that all Schlumberger soundings were carried out on young sea ice. Multiyear ice was unfortunately not met on the profile.
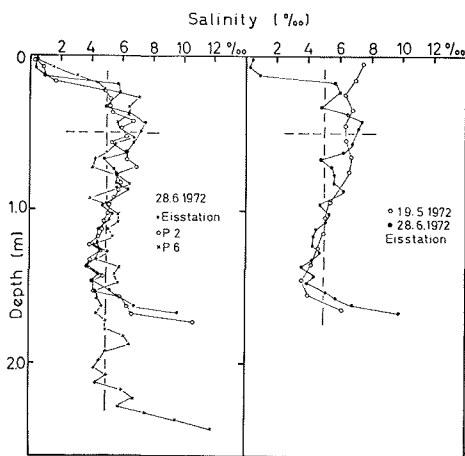

Fig. 6: Salinity distribution within the sea ice at different sites and different times.

Abb. 6: Die Salinität des Meereises in Abhängigkeit von der Tiefe an verschiedenen Orten und zu verschiedenen Zeiten.

122

The resistivities of both layers show a monotonic decrease with time (Fig. 3b). This process becomes especially evident when averaging the resistivities (Table 1) as well as the apparent resistivities (Fig. 5) for each run. It is obvious that an increase in brine due to the temperature increase reduces the resistivities as implied above. The heating of the ice from outside affects especially the upper layer (Fig. 5).

To eliminate all disturbances from outside the ice as much as possible, the following calculations are restricted to the second layer (depth $<$ 0,5 m). Because of the varying macrostructure of the ice the resistivities still scatter too much and it is hardly possible to relate the resistivities to the temperatures. Therefore, the resistivities of each run are smoothed by averaging five values at times. Figure 7 shows the smoothed values along the profile. The curves are extrapolated from P4 to P2 by the aid of the single values. The resistivities increase markedly from the costal stations to the centre part of the sound due to the temperature decrease in the ice in this direction. During the warming of the ice cover this effect diminished rapidly.
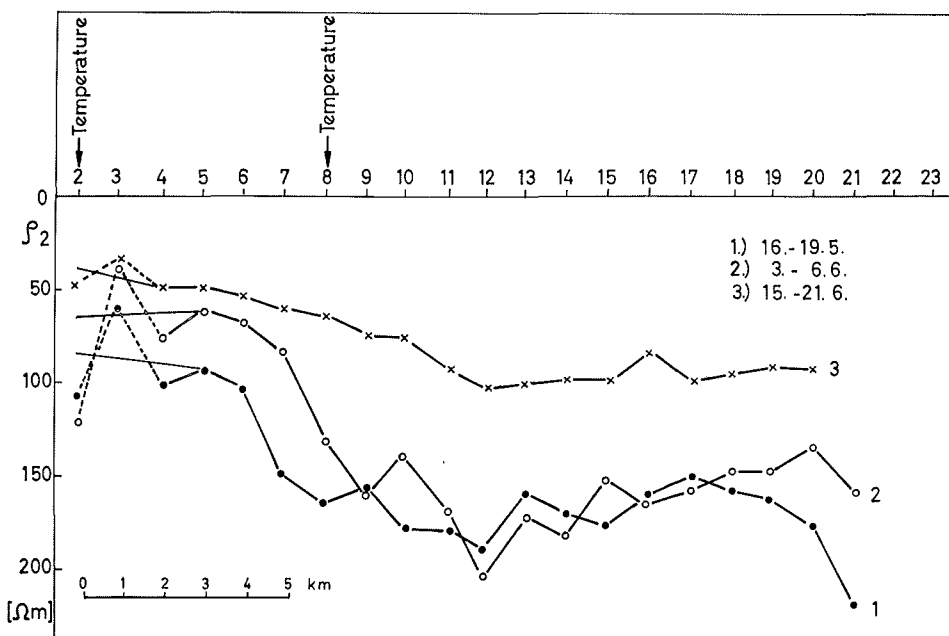

Fig. 7: Smoothed resistivities of the second layer along the profile (the curve is extrapolated between P2 and P4).
Abb. 7: Geglättete Widerstände der zweiten Schicht aufgetragen gegen das Profil (extrapoliert zwischen P2 und P4).

In Figure 8, the resistivities ϱ_{2m} of the sites P2 and P8, where the temperatures in the ice are known (Kohnen, 1972; Werner et al., 1972), are plotted versus the temperatures. Unfortunately, the temperature of the last run is missing at P2 because meltwater brought the measurements to an end. By reason of the limited number of values ϱ_{2m} it is not reasonable to derive a quantitative relation for ϱ_{2m} (T), but the resistivities can be compared with a theoretical model.

The conductivity of sea ice depends on the porosity, the saturation of the pores with brine and the conductivity of the brine. The ice matrix and the air inclusions — treated here as a part of the matrix — can be neglected because their conductivity is extremly
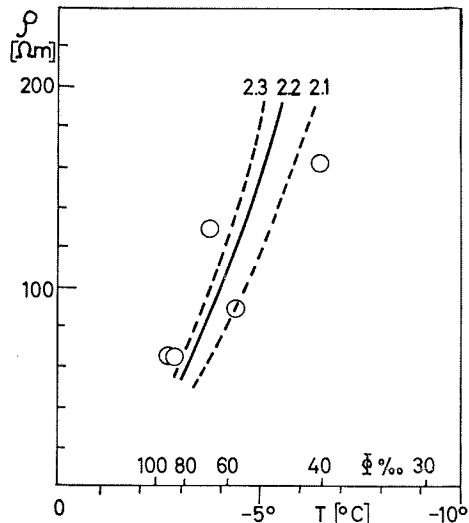
123

Fig. 8: Smoothed resistivities of the second layer versus temperature and porosity compared with resistivities calculated after equ. 3 (Archie) with different exponents n.

Abb. 8: Geglättete Widerstandswerte der zweiten Schicht in Abhängigkeit von der Temperatur und Porosität, verglichen mit nach Archie berechneten Werten für verschiedene Exponenten n.

low. Since the pores are saturated with brine the porosity Φ corresponds to the brine volume b. Thus, the resistivity can be derived from

3) $\varrho = a\Phi^{-n} \cdot \varrho_b$ (Archie, 1942)

where ϱ is the bulk resistivity, Φ is the porosity (fraction per unit volume), ϱ_b is the resistivity of brine and "a" and "n" are parameters depending on the structure of the material. "a" varies only slightly from less than 1 and a value of 1 may be assumed. The exponent n is about 2 or somewhat larger than 2 for well cemented granular materials. Thus, the resistivity of the sea ice is controlled by the brine content and its resistivity which, in turn, are temperature dependent. Especially the brine content is extremly sensitive to temperature variations.

From the mean salinity of the second layer S $=$ 5$^0/_{00}$ and the temperature T $= -5^\circ$C the brine volume b $=$ 5,6$^0/_0$ is obtained by applying the relation of Frankenstein and Garner (1967). The salinity is taken constant over the investigation period and along the profile because repeated salinity measurements and measurements at different sites (Fig. 6) did not show significant differences. The values of S and b yield a concentration of 90 g/l for the brine inclusions. The resistivities of solutions of the components of sea ice with such concentration lead to an estimation of $\varrho_b = 0,2 \, \Omega$ m at -5°C (after Keller and Frischknecht, 1966). The temperature dependance of ϱ_b is eliminated by applying

4) $\varrho_b \, (t) = \varrho_c \, e^{\frac{E}{kt}}$

where ϱ_c is a constant, k is the Boltzmann's constant, t ist the absolute temperature and E the activation energy. E $=$ 0,2 eV is taken as upper limit of the activation energy (Hochstein, 1965). Since ϱ_b (T) varies not more than by 15$^0/_0$ within the temperature range met during the measurements (Table 2) it's influence is about almost neglegible compared with Φ^{-n} (T) which varies by some hundred percent (Table 2).

Agreement between measured and theoretical resistivities is found for n $=$ 2,2 (Fig. 8). This result is consistent with what we might expect for a well cemented granular medium indicating also that the model (equ. 3) is appropriate to describe the conductivity behaviour of sea ice.

124

Run	Location	T [°C]	Φ ⁰/oo	ϱ_{2m} [Ωm]
2	P2	—2,7	90	65
1	P2	—4,4	57	84
3	P8	—3,0	82	64
2	P8	—3,7	67	132
1	P8	—6,5	40	165

Tab. 2: Resistivities, temperatures and porosities of the second layer ($\Phi = b$ is determined by using the relation of Frankenstein and Garner, 1967).
Tab. 2: Spezifische Widerstände, Temperatur und Porosität der zweiten Schicht ($\Phi = b$ wurde nach der Beziehung von Frankenstein und Garner, 1967 bestimmt).

The average brine volume can also be determined from seismic measurements using Wyllie's relation:

$$5) \quad \frac{1}{V} = \frac{\Phi}{V_L} + \frac{1-\Phi}{V_M} \qquad \text{(Wyllie et al., 1956)}$$

where V is the mean P-wave velocity in the ice, V_M the matrix velocity of the pure ice, V_L the velocity in the brine at the given temperature and Φ the porosity. With $V = 3,52$ km/sec (deduced from seismic data (Kohnen, 1972), of the shear and plate wave velocities), $V_L = 1,53$ km/sec and $V_M = 3,80$ km/sec equation (5) yields a porosity $\Phi = 5,6^0/o$ which is actually the same value as determined from the salinity and temperature measurements. When discussing the Archie relation we could neglect the air inclusions because of their low conductivity. Using Wyllie's formula this is generally not admissible because a large portion of air inclusions could affect seriously the bulk velocity of the sea ice. However, the influence of the air inclusions upon the velocities is well known. At a density of about 0,91 g/cm³, the entrapped air does not affect the velocities by more than $0,5^0/o$ which may be neglected. Thus, the agreement between the porosities determined from seismic and salinity-temperature measurements is satisfying within the limits of error and also the seismic velocities suggest that we may set here $\Phi = b$.

Conclusions

Numerous Schlumberger dc resistivity soundings were carried out on the sea ice near Pond Inlet, N. W. T. in the spring 1972 to investigate the anisotropy of the ice and to determine the resistivity and its temperature and time dependence. All curves of the apparent resistivity show the same typical feature indicating that a simple three-layer-case is an adequate model for the ice cover and the infinite half space of the sea water. Only young ice was met during the measurements as seen from the salinities and resistivities which are all of the order of magnitude of 10^2 Ω m. No indications of a significant and systematic azimuthal variation of the resistivity was found. Thus, the sea ice could be regarded as transversely isotropic with its main axis parallel to the vertical arrangement of the brine cells. The coefficient of anisotropy ($\lambda = 0,26$) was determined from measurements perpendicular and parallel to the surface on the wall of a pit dug into the ice. The equivalent ice thickness h_e calculated from the resistivity soundings are accordingly too small compared with the true depth H obtained from drilling. λ can also be derived from h_e and H. However, these coefficients scatter considerably but show a systematic trend along the profile which can be related to the macrostructure of the ice cover. Ridges, rafted ice, a distinct bottom morphology and fractures alter the conditions required for the Schlumberger method resulting in a large scatter of the equivalent thickness. These structures act to disorient the main direction of the anisotropy and consequently tend to make the medium behave isotropic. The coefficient of undisturbed ice, which is approximately 0,3, is close to the pit value whereas a heavily disturbed

ice cover appears nearly isotropic. There is no evidence for a temperature dependence of λ.

The resistivities from the Schlumberger soundings correspond to the mean resistivities ϱ_m. Despite a serious scatter, which is due to the same sources as discussed above, ϱ_m decreased markedly with time. It is a rise of the temperature by not more than 4°C which produces the decrease of ϱ_m. The bulk resistivity of a porous material with interconnected pore space, whose matrix is a semiconductor and whose liquid component is an electrolyte, is controlled by the resistivity of the liquid component. The porosity of the sea ice correponds to the brine volume because the pores are saturated with brine and the air bubbles can be neglected. The brine content as well as its resistivity are temperature dependent. The theory of Archie provides an adequate model for the conductivity in sea ice, and resistivities are calculated from the salinity and the temperature using Archie's law. Calculated and measured resistivities are consistent.

References

1. A c k l e y , S. F. , A. I. G o w , F. K u g z r u k and D. L a n g s t o n , 1974 : Physical Properties of Salt and Lake Ice in Relation to Microwave Measurements of Ice Thickness. Technical Note, U.S.A. CRREL, Hanover, N. H.
2. A r c h i e , G. E. , 1942 : The electric resistivity log as an aid in determining some reservoir characteristics. J. Petrol. Technol., 5, S. 1.
3. B h a t t a c h a r y a , P. K. and H. P. P a t r a , 1968 : Direct Current Geoelectric Sounding. Elsevier Pub. Co., Amsterdam.
4. D e p p e r m a n n , K. , H. F l a t h e , F. H a l l e n b a c h und J. H o m i l i u s , 1961 : Die geoelektrischen Verfahren der angewandten Geophysik. In A. Bentz (ed.): Lehrbuch der Angewandten Geologie, Bd. I, pp. 718—804. Enke Verl., Stuttgart 1961.
5. F r a n k e n s t e i n , G. and G. G a r n e r , 1967 : Equations for Determining the Brine Volume of Sea Ice from — 0,5° C to — 22,9° C. J. of Glaciol., Vol. 6, No. 48, pp. 943—944.
6. H o c h s t e i n , M. , 1965 : Elektrische Widerstandsmessungen auf dem grönländischen Inlandeis. Meddelser om Grønland, Bd. 177, Nr. 3.
7. K e l l e r , G. V. and F. C. F r i s c h k n e c h t , 1966 : Electrical Methods in Geophysical Prospecting. Pergamon Press, New York.
8. K o h n e n , H. , 1972 : Seismic and ultrasonic measurements on the sea ice of Eclipse Sound near Pond Inlet, N.W.T. on northern Baffin Island. Polarforschung, Jg. 42, No. 2, pp. 66—74.
9. W a l t e r , R. and K. B l e w e t t , 1972 : Strukturkartierung und Profilaufnahme im Meereis des Eclipse Sound (Baffin Island). Polarforschung, Jg. 42, No. 2, pp. 97—101.
10. W e r n e r , J. , B. T. S c h r e i n e r and E. T r e u d e , 1972 : Meteorologisch-geländeklimatologische Untersuchungen bei Pond Inlet, N.W.T. (Baffin Island). Polarforschung, Jg. 42, No. 2, pp. 102—109.
11. W y l l i e , M. R. I. , A. R. G r e g o r y and L. W. G a r d n e r , 1956 : Elastic Wave Velocities in Heterogeneous and Porous Media. Geophysics, 21, pp. 41—70.